AGGLOMERATED Co-Cr/SBA-15 CATALYSTS FOR HYDROGEN PRODUCTION TROUGHT ACETIC ACID STEAM REFORMING

J.A. Calles, A. Carrero, A.J. Vizcaíno, P.J. Megía
Chemical and Energy Technology Department, ESCET, Rey Juan Carlos University
C/Tulipán s/n, 28933, Móstoles (Madrid), Spain.
Corresponding author: Alicia Carrero, e-mail: alicia.carrero@urjc.es

REFERENCE NO

HYPR-04

Keywords:
Co-Cr/SBA-15
Agglomeration
Extrusion
Hydrogen production

ABSTRACT

Extruded Co-Cr/SBA-15 were performed to be tested in acetic acid steam reforming as a new catalysts to adapt this process up to industrial scale. Prepared samples were characterized by N_2 physisorption, ICP-AES, XRD, H_2-TPR and TGA. Catalyst/bentonite ratio was modified in order to improve the catalytic performance and the mechanical strength of the pellets. Bentonite addition led to decrease the S_{BET} and to improve the crushing strength. Reaction results showed that the catalyst that achieved the best catalytic results in terms of conversion and hydrogen production was the sample with lower amount of binder but it presented the lowest mechanical resistance forming high amount of fines during the reaction. Since the sample with 25 wt.% of bentonite seems to reach an equilibrium between H_2 production, conversion and crushing strength it was selected as the best extruded catalyst.

1. INTRODUCTION

High emission rate of greenhouse gases as well as solid particles derived from the use of fossil fuels as energy carrier contribute to global pollution and they are a limited resource. Between many alternatives, hydrogen nowadays is becoming an interesting energy source fuel because only water is produced when it is used in energy applications [1, 2]. Hydrogen can be obtained from fossil fuels, water and biomass using different methods [3-8]. At industrial scale, it is mainly produced from hydrocarbons, which are neither sustainable or renewable. Therefore, it is necessary to search for other alternatives to these fuels in order to decrease or dismiss the global contamination. Hydrogen production from biomass-derived products, such as bio-oils, oxygenated hydrocarbons (bio-oil aqueous fraction, bioalcohols, etc.), alkanes and bio-alcohols, is a remarkable alternative to these fossil fuels.

Fast biomass pyrolysis is becoming a quite interesting chance because bio-oil produced is considered a potential source of hydrogen [9]. By water addition, this bio-oil turn on two different fractions: an organic one to be used for biofuels production and a low value aqueous fraction. Bio-oil aqueous fraction can increase its value by hydrogen production through catalytic steam reforming. The overall equation of this process is as follows:

$$C_nH_mO_k+(2n-k)H_2O \rightarrow nCO_2+(2n+m/2-k)H_2$$

Bio-oil aqueous fraction usually presents different and complex compositions, which depends on the raw material used as biomass source for the bio-oil production (lignocellulosic waste or microalgae biomass) [10-14]. Regardless the raw material, in general terms, it is easy to find carboxylic acids, furans, ketones, phenols, etc. Due to the complex composition of bio-oil aqueous fraction, many research groups focus firstly their studies on the steam reforming of bio-oil model compounds [10, 11, 15-17]. Among the main compounds found in bio-oil aqueous fraction, acetic acid used to be in high concentration (around 20 wt. %) when bio-oil is produced from biomass fast pyrolysis [10, 11]. Moreover, acetic acid compared with other hydrogen sources such as methanol and ethanol, is non-flammable and much safer to store and transport [18].

Established and developing technologies used to produce hydrogen can be classified in three different groups: the first one is a technology with net positive emission of CO and CO_2, the second one is with CO_2 free emissions and the last one with CO_2 neutral emission. Steam reforming of oxygenated hydrocarbons as acetic acid is included in carbon neutral process because the CO_2 produced during the process will be consumed by next biomass generations.

In steam reforming processes, the catalyst plays a crucial role where deactivation due to coke deposition or sintering, together with maximizing hydrogen selectivity. Noble metals based catalysts are usually reported as active catalysts [1, 18] but they involves high cost. In addition, transition metals such as Ni or Co showed good performance for use in catalytic steam reforming and they are cheaper than noble metals [1]. While Ni has been widely reported as active phase for steam reforming, Co has caused less attention despite it provides high catalytic activity at lower temperatures where water gas shift reaction is favoured, increasing hydrogen production [19].

In our previous work [20] Co-based catalysts were synthetized in order to use them for catalytic glycerol steam reforming. Results showed how Co/SBA-15 catalysts suffer a severe conversion drop along the time leading to the possibility to improve. To avoid that conversion decay, it is possible to incorporate promoters. Casanovas *et al.* [21], achieved better catalytic performance towards ethanol steam reforming using Cr as promoter in Co-based catalysts. In previous works, a screening of promoters in Co-based catalysts was done [22], and the addition of Cr leaded to the highest enhancement of catalytic activity in terms of hydrogen production (around 50% v/v) and it achieved the lowest concentration of gaseous carbon products.

The inconvenience in the vast majority of the catalysts used in steam reforming research is that they are usually prepared as fine powders being not appropriate for use in fixed bed reactors at industrial scale because of the high pressure drop caused by the catalyst.

In general, this is solved using pelletized materials, which are manufactured with the inclusion of binders [23, 24]. Extrudates are commonly manufactured with the addition of an inorganic binder such as bentonite, attapulgite, kaolin or sepiolite to enhance the strength, and an organic additive like methylcellulose or hydroxyethyl cellulose to enhance the viscosity of the paste during the extrusion [24, 25]. Nevertheless, no reports about the preparation of agglomerated Co-based catalysts for steam reforming can be found. Therefore, the aim of this work is the synthesis of new extruded Cr-doped Co-based catalyst for it use in acetic acid steam reforming (AcASR) using bentonite as binder and methylcellulose as organic additive, studying the effect of the bentonite/catalyst ratio.

2. EXPERIMENTAL WORK

2.1. Catalysts preparation

Synthesis of SBA-15 was done following the hydrothermal method described elsewhere [26]. The incorporation of active phase and promoter was done following the incipient wetness impregnation using the corresponding nitrate solution to achieve 7 wt.% of active phase and 2 wt.% of promoter in the final catalyst. Afterwards samples were calcined at 550ºC in static conditions for 5h (1.8 °C/min heating rate).

Extruded materials were prepared following the methodology reported by Pariente *et al.* [24]. The procedure is as follows: powder catalyst (70-80 wt.%) was blended with sodium bentonite (20-30 wt.%) as inorganic binder to increase the mechanical strength of extrudates and synthetic methylcellulose polymer (10 wt.% over the mixture) to improve the viscosity of the paste during the extrusion [23]. All components were mixed up with deionized water to get a homogeneous paste. Afterwards, the paste was placed in a damp atmosphere, which provides plasticity and cohesive properties to be easily extrudable [24]. After that, the paste was extruded through a 2.8 mm circular die using

a homemade extruder. Pellets were obtained by crushing the extruded material until particle sizes around 2 mm that were appropriate to be use in a fixed bed reactor.
Finally, these pellets were firstly dried at 110°C for 3h with a heating rate of 0.1°C/min and secondly, calcined at 650ºC (0.5°C/min) for 2h in order to eliminate the organic additive. Samples were named as Co-Cr/SBA-15 (X), where X corresponds to the amount of bentonite in terms of wt.%.

2.2. Catalytic tests

Acetic acid steam reforming reactions were performed on a MICROACTIVITY-PRO unit (PID Eng & Tech. S.L.) as described in previous works [20, 27]. The reactions were carried out isothermally at 600ºC and atmospheric pressure. All catalysts were previously reduced under pure hydrogen (30 mL/min) at 600°C during 6.5h with a heating rate of 2 °C/min according to H_2-TPR results. Reaction feed was a mixture of acetic acid and water using steam/carbon (S/C) molar ratio of 2 and WHSV = 30 h^{-1} defined as the ratio between the inlet feed and the mass of the catalyst. The composition of the gas effluent was measured online with a in an Agilent (Santa Clara, CA, USA) 490 Micro-GC equipped with a PoraPlot U column (10 m), a molecular sieve 5A column (20 m) and a thermal conductivity detector (TCD). Condensable vapours were trapped in the condenser at 4 °C and analysed in a Varian (Palo Alto, CA, USA) CP-3900 chromatograph equipped with a CP-WAX 52 CB (30 m × 0.25 mm, DF = 0.25) column and flame ionization detector (FID). Carbon deposited during catalytic tests was evaluated by thermogravimetric analyses (TGA) performed in air flow (100 Ncm^3/min) on a TA Instruments (New Castle, DE, USA) SDT 2960 thermobalance, with a heating rate of 5 °C/min up to 800 °C.

2.3. Catalysts characterization

The textural properties of prepared materials were measured by N_2 adsorption/desorption at 77 K on a Micromeritics TRISTAR 3000 sorptometer. Samples were previously outgassed under vacuum at 200 °C for 4 h. Standard deviations in BET surface area and pore volume measurements are 1.1 m^2/g and 0.02 cm^3/g, respectively.
ICP-AES technique was used to determine the chemical composition of the catalysts, using a Varian VISTA-PRO AX CCD-Simultaneous ICP-AES spectrophotometer (relative standard deviation: 0.5%). Previously, solid samples were dissolved by acidic digestion.
XRD measurements were recorded using a Philips X'pert Pro diffractometer using Cu $K\alpha$ radiation.
Reducibility of the samples was studied by means of TPR experiments. These were performed on a Micromeritics AUTOCHEM 2910 equipment by passing a 10% H_2/Ar flow (35 N mL/min) through the sample (100 mg) and increasing temperature up to 980 °C at a heating rate of 5 °C/min. Samples were previously outgassed under Ar flow at 110 °C for 30 min.
TEM micrographs were obtained on a Philips TECNAI 20 microscope (200 kV) with a resolution of 0.28 nm. The apparatus has also the possibility to perform elemental microanalysis by EDX. Samples were prepared by suspending the material in acetone by ultrasonication and subsequent deposition on a carbon-coated copper grid.
Pellets strength was determined on a Chatillon DFS II using a compression mechanical standard test. The crushing strength was defined as the maximum force measured prior to fracture divided by the cross-sectional area of the pellet [28].

3. RESULTS AND DISCUSSION

3.1. Catalysts characterization

ICP-AES results are summarized in Table 1. As it can be seen, cobalt and chromium content in powder Co-Cr/SBA-15 catalyst is near to the nominal values. Attending to the extruded catalysts, metal content is lower due to the bentonite percentage. If it is recalculated on the basis of the catalyst, the results are similar to the powder catalyst.

Table 1. Metal content in catalysts determined by ICP

Sample	Co (wt.%)	Cr (wt.%)
Co-Cr/SBA-15	6.4	1.7
Co-Cr/SBA-15 (30)	4.5	1.2
Co-Cr/SBA-15 (25)	4.9	1.3
Co-Cr/SBA-15 (20)	5.3	1.4

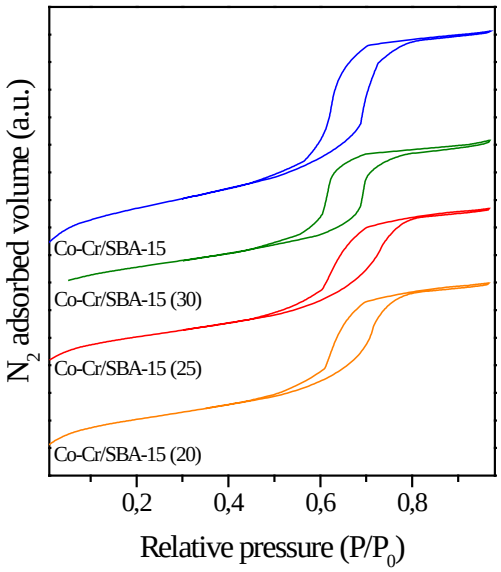

Figure 1. Nitrogen adsorption-desorption at 77K of calcined powder Co-Cr/SBA-15 and extruded materials.

Figure 1 shows the nitrogen adsorption-desorption at 77K of all samples. Powder catalyst present a type IV isotherm (according to the I.U.P.A.C. classification) with a H1-type hysteresis loop that indicates the preservation of the initial mesostructured support. The hysteresis loop is due to the process of filling the mesopores and it is governed by the phenomenon of capillary condensation and by the percolative properties of the solid. Regarding extruded materials, it can be determined that all present a type IV isotherm as well as the powder catalyst. On the other hand, when the amount of binder in catalysts becomes higher, the area becomes smaller between 27-34% comparing with the powder sample. It can be verified by calculating the textural properties, which are summarized in Table 2.

Table 2. Textural properties of Co-based catalysts.

	S_{BET} (m^2/g)	V_p (cm^3/g)	D_p (nm)
Co-Cr/SBA-15	490	0.7	55
Co-Cr/SBA-15 (30)	322	0.5	54
Co-Cr/SBA-15 (25)	335	0.5	58
Co-Cr/SBA-15 (20)	355	0.5	58

Metal dispersion in calcined Co-Cr/SBA-15 powder can be observed in Figure 2. The well-ordered hexagonal array of cylindrical channels are in accordance with the N_2 physisorption isotherm. Dark zones observed on the mesoporous structure of SBA-15 correspond to mixed cobalt and chromium oxides nanoparticles placed over the external surface as could be proved in EDX analysis (not shown). Other smaller particles can also be observed with an irregular shape that seems to be adapted to the support pores shape.

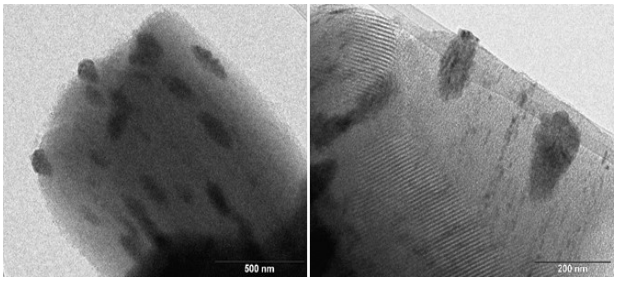

Figure 2. TEM images of the calcined powder Co-Cr/SBA-15.

The H_2-TPR results obtained for powder Co-Cr/SBA15 (see Figure 3) presents a first zone, which has two peaks with maximum located at 205 and 270ºC. Since Cr has lower reduction temperatures than Co [29-32], the contribution of this metal to the first reduction zone should be higher. The feature with maxima at 517ºC corresponds to Co oxide species with a stronger interaction degree with the support. Attending to the extruded materials, the peak around 205º disapears and the peak over 270ºC leads to higher temperature. Since Co loading is higher than Cr, it is possible to assume that most chromium may be involved in a mixed oxide [33], probably due to the higher calcination

temperature of extruded samples, which was 100ºC above powder catalyst. The shoulder around 517ºC found in the powder catalysts moves to lower temperature indicating less interaction with the support [31] due to the presence of bentonite.

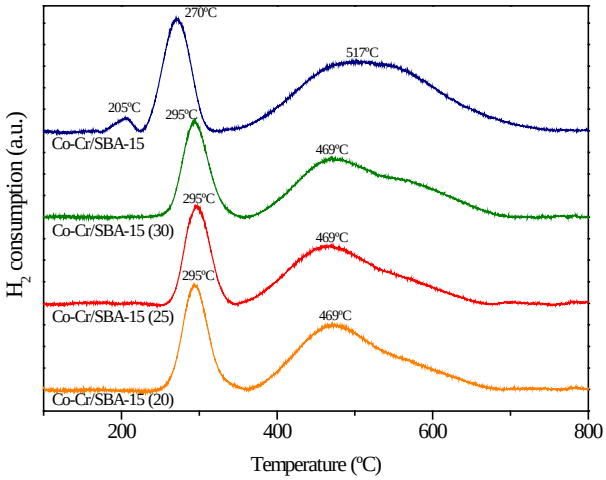

Figure 3. H_2-TPR profiles of the calcined powder Co-Cr/SBA-15 and extruded materials.

Figure 4 shows the X-ray patterns of calcined samples. Powder Co-Cr/SBA-15 shows a wide peak between 20-30º attributed to the amorphous silica forming the walls of the support pores. Attending to cobalt presence, peaks of Co_3O_4 phase (JCPDS 43-1003) can be observed at different positions: 31.2, 36.5, 44.5, 55.3, 58.9, 64.6, 71.6 and 77.2º, which can be assigned to the (220), (311), (400), (422), (511), (440), (442) and (533) diffraction planes respectively, according to the XRD pattern of Co_3O_4 cubic crystalline. No peaks corresponding to chromium species were detected due to the low concentration of this metal in the samples. In extruded materials, the same phase of Co appears at the same positions as in the powder catalyst, but new peaks appear at 26.66, 28.02, 34.59 and 60.67º. Theses peaks are attributed to the presence of bentonite used as blinder in the extruded materials. Specifically these peaks correspond to montmorillonite (JCPDS 00-013-0135), which used to be the main compound of bentonite, with quartz as impurity [34].

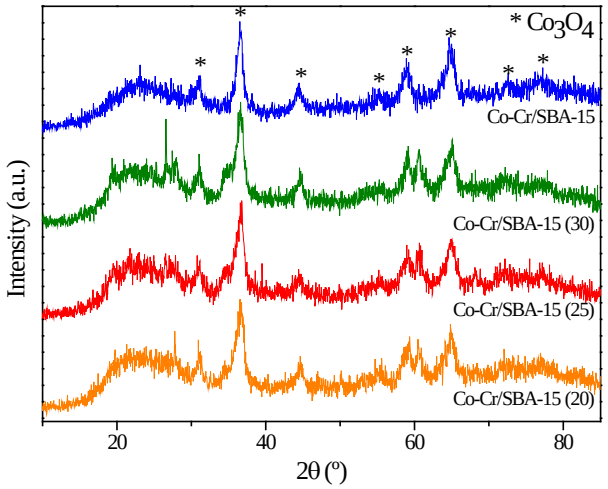

Figure 4. Comparison of XRD patterns of Co-Cr/SBA-15

3.2. Catalytic tests

In previous work, powder Co-Cr/SBA-15 achieved a yield around 50% of H_2 v/v, up to 98% of AcA conversion and coke produced was 37 wt.% [22]. In that work, between all tested catalysts Co-Cr/SBA-15 achieved the best performance in AcASR. This is in concordance with Casanovas *et al.* [21]. Their results showed that Cr incorporation was related with the better catalytic performance in ethanol steam reforming.

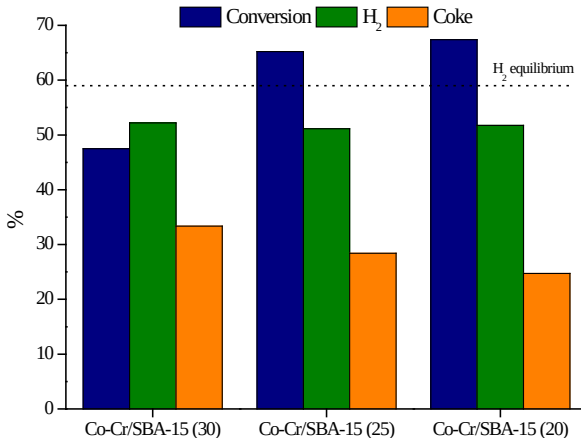

Figure 5. Catalytic results for extruded catalysts. Conversion (mole %), H2 (% v/v) and Coke (wt.%).

Obtained results in AcASR reactions using the extruded materials are shown in Figure 5. As it can be observed, similar results were obtained in terms of hydrogen production achieving around 50% in the outlet stream in all cases. This value is next to that obtained with the powder catalyst [22]. Conversion

becomes higher when the metal content increase in each sample but all of them are below the one obtained with Co-Cr/SBA-15. It can be associated to the fact that extruded materials have lower content of active phase due to the bentonite incorporation.

As all reactions were carried out with the same amount of extruded catalysts, reactions didn´t have the same amount of cobalt. For this reason, other values of TOF (turnover frequency) and H_2 content in the outlet stream were calculated using equations (1) and (2). TOF for powder catalyst was 44.68 h^{-1} which value is next to the obtained by the sample with lower amount of bentonite. Table 3 summarizes the obtained results in terms of hydrogen content and TOF.

Table 3. TOF and H_2 production in catalysts.

TOF (h^{-1})		
Co-Cr/SBA-15 (30)	Co-Cr/SBA-15 (25)	Co-Cr/SBA-15 (20)
31.48	38.75	40.93
H_2 (mole)		
Co-Cr/SBA-15 (30)	Co-Cr/SBA-15 (25)	Co-Cr/SBA-15 (20)
$0.25 \cdot 10^{-2}$	$0.27 \cdot 10^{-2}$	$0.26 \cdot 10^{-2}$

At first, the best-selected catalyst/binder ratio must be the one with the highest conversion and hydrogen production. However, for use a catalyst at pilot plant or industrial scale, it is necessary to considerate that particles with a low mechanical strength may break in the reactor or during transport and storage, leading to the formation of fragments and fines, which can cause various problems for the running of the industrial units [35].

Table 4 summarizes the crushing strength tests done to the extruded catalysts. Results were calculated as an average of five different analysis. Measurements were carried out to the pellet as shown in Figure 6. As can be determined from the results (Table 4), crushing strength become higher when the amount of binder increases. So, it is completely related to the amount of binder in the pellet having a pseudo-linear behaviour. Attending to crushing strength results, Co-Cr/SBA-15 (20) presents lower crushing strength than the others and it will broke easily during the reaction. In fact, when the catalyst was recovered after the reaction, some fines and broken particles were observed. Comparing all recovered catalysts, we can conclude that these fines appears in greater extent when the binder content was smaller.

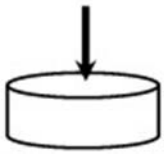

Figure 6. Pellet position for the strength analysis.

Table 4. Crushing strength results for the extruded catalysts.

	Crushing strength (kPa)
Co-Cr/SBA-15 (30)	417.84
Co-Cr/SBA-15 (25)	290.99
Co-Cr/SBA-15 (20)	183.28

It is known that under steam reforming conditions, water can react to remove some coke via gasification that may cause structural defects [36]. TGA can be used to determine the structural order of coke formed during the reaction because more ordered carbon structure will have higher gasification temperature [37]. Figure 7 shows the derivative thermograms (DTG) of all tested catalysts where it is possible to observe at what temperature the oxidation of coke took place. All samples present a similar DTG profile with a maximum around 500ºC and a small shoulder over 550ºC. In all cases, the formed coke is some kind of amorphous carbon because it is oxidized below 550ºC and filamentous or graphitic carbon does at higher temperature [38, 39]. The overlap between those two peaks indicates the same carbon specie with two different ordering degree.

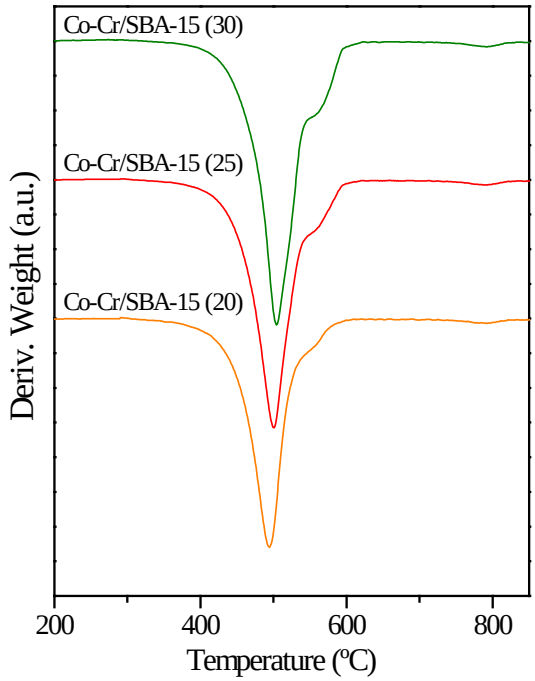

Figure 7. Derivative thermogravimetric (DTG) analysis of the extruded catalysts used in AcASR.

From all results, it is possible to conclude that the best catalytic performance in terms of conversion was achieved by the catalysts with the lowest amount of binder Co-Cr/SBA-15(20). Regarding crushing strength of all catalysts, this one is not appropriate for it use in our reaction condition, much less for use in pilot plant scale. Since Co-Cr/SBA-15 (25) seems to reach an equilibrium between H_2 production, conversion and crushing strength, it was selected as the best extruded catalysts. At future work, different calcination temperatures and different pellets size, will be tested in AcASR. In addition, regeneration cycles will be carry out in order to evaluate the durability of this new extruded catalyst.

4. EQUATIONS

$$TOF = \frac{\text{AcA converted (mole)}}{\text{t (h)}\cdot\text{Co amount (mole)}} \quad (1)$$

$$H_2 = \frac{H_2\ \text{(mole/h)}}{\text{TOF } (h^{-1})} \quad (2)$$

5. CONCLUSIONS

Co-Cr/SBA-15 extruded catalysts were prepared using bentonite as inorganic binder and methylcellulose as organic additive. A linear increase behaviour of crushing strength was observed as the amount of bentonite increased. The physicochemical properties of extrudates were slightly affected by the presence of bentonite. S_{BET} and active phase content were reduce, while the mesoporous structure of the powder catalyst was preserved in line with obtained type IV isotherms.

Extruded catalysts led a worse catalytic performance from the point of view of acetic acid conversion and hydrogen production comparing with the results obtained with the powder catalyst. This was attributed to the presence of bentonite since the WHSV was the same in all cases but not the metal content.

DTG results shows that all samples overlap two peaks indicating the same carbon specie with two different ordering degree. This carbon deposits were ascribed to some kind of amorphous carbon because its oxidation below 550ºC.

Reaction results showed the best catalytic results in terms of conversion and hydrogen production was the achieved with the sample with lower amount of binder but it presented the lowest mechanical resistance forming high amount of fines during the reaction. On the other hand, the sample with a medium content of binder seem to reach an equilibrium between H_2 production, conversion and crushing strength. Therefore, a 25 wt.% of bentonite was enough to obtain a good catalytic performance and a suitable mechanical resistance of the pellets.

Acknowledgements

Authors acknowledge the financial support from the Regional Government of Madrid (project S2013/MAE-2882) and from the Spanish Ministry of Economy and Competiveness (project CTQ2013-44447-R)

References

[1] Vizcaíno A.J., Carrero A., Calles J.A. *Hydrogen production from bioethanol*. New York: Nova Science Publishers; 2012 pp. 247-294.

[2] Agency I.E. Hydrogen Production and Storage: R&D Priorities and Gaps. Paris, France: IEA Publications; 2006.

[3] Ayalur Chattanathan S., Adhikari S., Abdoulmoumine N. A review on current status of

hydrogen production from bio-oil. *Renewable and Sustainable Energy Reviews*,Vol. 16, 2012, pp. 2366-72.
[4] Barca C., Soric A., Ranava D., Giudici-Orticoni M.-T., Ferrasse J.-H. Anaerobic biofilm reactors for dark fermentative hydrogen production from wastewater: A review. *Bioresource Technology*,Vol. 185, 2015, pp. 386-98.
[5] Chaubey R., Sahu S., James O.O., Maity S. A review on development of industrial processes and emerging techniques for production of hydrogen from renewable and sustainable sources. *Renewable and Sustainable Energy Reviews*,Vol. 23, 2013, pp. 443-62.
[6] Dincer I., Acar C. Review and evaluation of hydrogen production methods for better sustainability. *International Journal of Hydrogen Energy*,Vol. 40, 2015, pp. 11094-111.
[7] Gradisher L., Dutcher B., Fan M. Catalytic hydrogen production from fossil fuels via the water gas shift reaction. *Applied Energy*,Vol. 139, 2015, pp. 335-49.
[8] Ni M., Leung M.K.H., Leung D.Y.C., Sumathy K. A review and recent developments in photocatalytic water-splitting using TiO2 for hydrogen production. *Renewable and Sustainable Energy Reviews*,Vol. 11, 2007, pp. 401-25.
[9] Jacobson K., Maheria K.C., Kumar Dalai A. Bio-oil valorization: A review. *Renewable and Sustainable Energy Reviews*,Vol. 23, 2013, pp. 91-106.
[10] Remón J., Broust F., Volle G., García L., Arauzo J. Hydrogen production from pine and poplar bio-oils by catalytic steam reforming. Influence of the bio-oil composition on the process. *International Journal of Hydrogen Energy*,Vol. 40, 2015, pp. 5593-608.
[11] Remiro A., Valle B., Oar-Arteta L., Aguayo A.T., Bilbao J., Gayubo A.G. Hydrogen production by steam reforming of bio-oil/bio-ethanol mixtures in a continuous thermal-catalytic process. *International Journal of Hydrogen Energy*,Vol. 39, 2014, pp. 6889-98.
[12] Paasikallio V., Kihlman J., Sánchez C.A.S., Simell P., Solantausta Y., Lehtonen J. Steam reforming of pyrolysis oil aqueous fraction obtained by one-step fractional condensation. *International Journal of Hydrogen Energy*,Vol. 40, 2015, pp. 3149-57.
[13] Ji C., He Z., Wang Q., Xu G., Wang S., Xu Z., Ji H. Effect of operating conditions on direct liquefaction of low-lipid microalgae in ethanol-water co-solvent for bio-oil production. *Energy Conversion and Management*,Vol. 141, 2017, pp. 155-62.
[14] Du Z., Mohr M., Ma X., Cheng Y., Lin X., Liu Y., Zhou W., Chen P., Ruan R. Hydrothermal pretreatment of microalgae for production of pyrolytic bio-oil with a low nitrogen content. *Bioresource Technology*,Vol. 120, 2012, pp. 13-18.
[15] Calles J.A., Carrero A., Vizcaíno A.J., García-Moreno L. Hydrogen production by glycerol steam reforming over SBA-15-supported nickel catalysts: Effect of alkaline earth promoters on activity and stability. *Catalysis Today*,Vol. 227, 2014, pp. 198-206.
[16] Han X., Wang Y., zhang Y., Yu Y., He H. Hydrogen production from oxidative steam reforming of ethanol over Ir catalysts supported on Ce–La solid solution. *International Journal of Hydrogen Energy*,Vol. 42, 2017, pp. 11177-86.
[17] Mei Y., Wu C., Liu R. Hydrogen production from steam reforming of bio-oil model compound and byproducts elimination. *International Journal of Hydrogen Energy*,Vol. 41, 2016, pp. 9145-52.
[18] Chen G., Tao J., Liu C., Yan B., Li W., Li X. Hydrogen production via acetic acid steam reforming: A critical review on catalysts. *Renewable and Sustainable Energy Reviews*,Vol. 79, 2017, pp. 1091-98.
[19] Banach B., Machocki A., Rybak P., Denis A., Grzegorczyk W., Gac W. Selective production of hydrogen by steam reforming of bio-ethanol. *Catalysis Today*,Vol. 176, 2011, pp. 28-35.
[20] Carrero A., Vizcaíno A.J., Calles J.A., García-Moreno L. Hydrogen production through glycerol steam reforming using Co catalysts supported on SBA-15 doped with Zr, Ce and La. *Journal of Energy Chemistry*,Vol. 26, 2017, pp. 42-48.
[21] Casanovas A., Roig M., de Leitenburg C., Trovarelli A., Llorca J. Ethanol steam reforming and water gas shift over Co/ZnO catalytic honeycombs doped with Fe, Ni, Cu, Cr and Na. *International Journal of Hydrogen Energy*,Vol. 35, 2010, pp. 7690-98.
[22] Megía P.J., Carrero A., Calles J.A., Vizcaíno A.J. Influence of promoters addition to Co-based catalysts on acetic acid steam reforming. In preparation.
[23] Melero J.A., Iglesias J., Sainz-Pardo J., de Frutos P., Blázquez S. Agglomeration of Ti-SBA-15 with clays for liquid phase olefin epoxidation in a continuous fixed bed reactor. *Chemical Engineering Journal*,Vol. 139, 2008, pp. 631-41.
[24] Pariente M.I., Martínez F., Botas J.Á., Melero J.A. Extrusion of Fe_2O_3/SBA-15 mesoporous

material for application as heterogeneous Fenton-like catalyst. *AIMS Environmental Science*,Vol. 2, 2015, pp. 154-68.
[25] Chandrasekar G., Hartmann M., Palanichamy M., Murugesan V. Extrusion of AlSBA-15 molecular sieves: An industrial point of view. *Catalysis Communications*,Vol. 8, 2007, pp. 457-61.
[26] Zhao D., Feng J., Huo Q., Melosh N., Fredrickson G.H., Chmelka B.F., Stucky G.D. Triblock copolymer syntheses of mesoporous silica with periodic 50 to 300 angstrom pores. *Science*,Vol. 279, 1998, pp. 548-52.
[27] Carrero A., Calles J., García-Moreno L., Vizcaíno A. Production of Renewable Hydrogen from Glycerol Steam Reforming over Bimetallic Ni-(Cu,Co,Cr) Catalysts Supported on SBA-15 Silica. *Catalysts*,Vol. 7, 2017, pp. 55.
[28] Zakeri M., Samimi A., Afarani M.S., Salehirad A. Interaction between Weibull parameters and mechanical strength reliability of industrial-scale water gas shift catalysts. *Particuology*,Vol. 32, 2017, pp. 160-66.
[29] Yun D., Baek J., Choi Y., Kim W., Jong Lee H., Yi J. *Promotional Effect of Ni on a CrO_x Catalyst Supported on Silica in the Oxidative Dehydrogenation of Propane with CO_2*: ChemCatChem; 2012 pp. 1952–1959.
[30] Prieto G., Martínez A., Concepción P., Moreno-Tost R. Cobalt particle size effects in Fischer–Tropsch synthesis: structural and in situ spectroscopic characterisation on reverse micelle-synthesised Co/ITQ-2 model catalysts. *Journal of Catalysis*,Vol. 266, 2009, pp. 129-44.
[31] Prieto G., Martínez A., Murciano R., Arribas M.A. Cobalt supported on morphologically tailored SBA-15 mesostructures: The impact of pore length on metal dispersion and catalytic activity in the Fischer–Tropsch synthesis. *Applied Catalysis A: General*,Vol. 367, 2009, pp. 146-56.
[32] González O., Pérez H., Navarro P., Almeida L.C., Pacheco J.G., Montes M. Use of different mesostructured materials based on silica as cobalt supports for the Fischer–Tropsch synthesis. *Catalysis Today*,Vol. 148, 2009, pp. 140-47.
[33] Zoican Loebick C., Derrouiche S., Fang F., Li N., Haller G.L., Pfefferle L.D. Effect of chromium addition to the Co-MCM-41 catalyst in the synthesis of single wall carbon nanotubes. *Applied Catalysis A: General*,Vol. 368, 2009, pp. 40-49.
[34] Zhirong L., Azhar Uddin M., Zhanxue S. FT-IR and XRD analysis of natural Na-bentonite and Cu(II)-loaded Na-bentonite. *Spectrochimica Acta Part A: Molecular and Biomolecular Spectroscopy*,Vol. 79, 2011, pp. 1013-16.
[35] Li Y., Li X., Chang L., Wu D., Fang Z., Shi Y. Understandings on the scattering property of the mechanical strength data of solid catalysts: A statistical analysis of iron-based high-temperature water-gas shift catalysts. *Catalysis Today*,Vol. 51, 1999, pp. 73-84.
[36] Qi X., Guo X., Zheng C. Density functional study the interaction of oxygen molecule with defect sites of graphene. *Applied Surface Science*,Vol. 259, 2012, pp. 195-200.
[37] Chen J., Yang X., Li Y. Investigation on the structure and the oxidation activity of the solid carbon produced from catalytic decomposition of methane. *Fuel*,Vol. 89, 2010, pp. 943-48.
[38] Choong C.K.S., Zhong Z., Huang L., Wang Z., Ang T.P., Borgna A., Lin J., Hong L., Chen L. Effect of calcium addition on catalytic ethanol steam reforming of Ni/Al2O3: I. Catalytic stability, electronic properties and coking mechanism. *Applied Catalysis A: General*,Vol. 407, 2011, pp. 145-54.
[39] Galetti A.E., Gomez M.F., Arrúa L.A., Abello M.C. Hydrogen production by ethanol reforming over NiZnAl catalysts: Influence of Ce addition on carbon deposition. *Applied Catalysis A: General*,Vol. 348, 2008, pp. 94-102.